arXiv:2506.02632v1 [physics.optics] 3 Jun 2025

Phase Topology Stability of an Optical Vortex via an Electrically Controlled Twist-Planar Oriented Liquid Crystal Fresnel Lens

Elena Melnikova[1], Katsiaryna Pantsialeyeva[1], Dmitry Gorbach[1], Alexei Tolstik[1], Sergei Slussarenko Jr.[2], Alina Karabchevsky[3,4*]

[1]Department of Laser Physics and Spectroscopy, Belarusian State University, Minsk, Belarus.
[2]Griffith University, Brisbane, Australia.
[3*]School of Electrical and Computer Engineering, Ben-Gurion University of the Negev, Beer-Sheva, 8410501, Israel.
[4*]Department of Physics, Lancaster University, Lancaster, LA1 4YB, United Kingdom.

*Corresponding author(s). E-mail(s): a.karabchevsky@lancaster.ac.uk;
Contributing authors: Melnikova@bsu.by; pantsialeyevakate@gmail.com; gorbachdv@yandex.ru; Tolstik@bsu.by; s.slussarenko@griffith.edu.au;

Abstract

Optical vortices (OVs) have emerged as a revolutionary concept in modern photonics, offering a unique method of manipulating light beyond conventional Gaussian beams. Despite their vast potential, phase topology stability remains unaddressed, limiting their widespread adoption and performance in real-world environments. Here, we reveal the missing link to assessing the stability of optical vortices using an electrically tunable twist-planar liquid crystal (LC) Fresnel lens. The proposed LC-based lens leverages the birefringence and voltage-controlled reconfigurability of liquid crystals to dynamically probe the phase topology of singular beams. By modulating the LC orientation with an applied voltage, we restructure the optical phase in real-time without requiring modifications to the optical setup. The 3V and 35V voltage supply allows for the switch between the "topological charge detection" and "optical singular beam propagation" modes. This eliminates the need for additional optical elements, significantly simplifying the detection and characterization of vortex beams. Experimental and theoretical investigations demonstrate that the vortex topology can be unambiguously

identified from the intensity profile observed in the Fourier plane of a lens. Furthermore, the designed device features low power consumption, compact form factor, and seamless integration potential, making it a promising candidate for scalable vortex-based photonic systems.

Keywords: phase singular beam, optical vortex stability, topological charge, nematic liquid crystal

Main

Since their discovery, optical vortices (OVs) — phase singular beams characterized by helical phase front and carrying orbital angular momentum (OAM), provide transformative applications in optical communication, quantum information processing, high-resolution imaging, and laser-material interactions [1–7]. A defining feature of these beams is the presence of a phase singularity. At this point, the optical phase remains undefined, encircled by a helical phase structure that varies by $2\pi\ell$, where ℓ denotes the topological charge of the vortex. This helical phase profile imparts an intrinsic OAM to the beam, a property that has led to breakthroughs in optical communication [8, 9], optical manipulation of microobjects, and the study of rheological properties through angular momentum transfer [10, 11]. Optical vortices also play a pivotal role in astronomical imaging [12, 13], enabling high-contrast observations of exoplanets.

Another fundamental characteristic of vortex beams is the presence of a central intensity null due to the phase singularity. This property is exploited in applications such as solar coronagraphy [14, 15], high-precision laser material processing [16, 17], optical trapping and controlled micro-particle motion [18], and ultra-high-resolution microscopy [19, 20].

Various techniques have been developed to generate optical vortices, each leveraging different physical mechanisms. These include astigmatic mode conversion [21], spiral phase plates [22, 23], q-plates [24–27] and dynamically programmable wavefront shaping using spatial light modulators [28] and digital micromirror devices [29], photonic disclination cavities [30]. In the early 1990s, researchers began investigating the use of diffractive optical elements to generate optical vortices from beams with uniform phase fronts [31, 32]. A seminal study by Soskin, Vasnetsov, and Bazhenov demonstrated that introducing an optical dislocation into the grating structure—forming what are now known as fork or branched gratings—leads to the emergence of phase singularities in the diffracted beam [31]. This foundational work remains a cornerstone in the field of singular optics.

However, in practical systems, the stability of high-order optical vortices ($|\ \ell\ | > 1$) is fundamentally limited by imperfections in vortex generation techniques and the unavoidable presence of coherent background fields due to transmission, scattering, and reflection [21, 33, 34]. These perturbations introduce instability in the phase singularities of high-order vortices, leading to their fragmentation into multiple first-order vortices ($|\ \ell\ | = 1$) [33, 35]. This effect manifests as a transformation of the vortex

intensity distribution, with the appearance of multiple zero-intensity regions in the far field. While the singularity points may remain coalesced in the near field, particularly within the Rayleigh range, the presence of even a weak coherent background field in the far field induces significant separation of these singularities, with the degree of fragmentation increasing for higher topological charges [33, 35].

Here, we exploit the inherent instability as a means of directly determining the topological charge of optical vortices. By applying a Fourier transform via a focusing lens, we transfer the field's intensity distribution from the Fraunhofer region to the Fourier plane, greatly simplifying the experimental setup.

Several established methods exist for measuring the topological charge of optical vortices, including astigmatic transformations via tilted or cylindrical lenses [36–38], spatial light modulators [39], diffraction through gratings [40, 41] or structured apertures [42, 43], as well as interference-based techniques [44, 45]. While effective, these approaches typically require the use of additional optical components in the beam path, complicating experimental setups and limiting real-time applications where simultaneous vortex generation and measurement are required.

Here, we propose a novel approach that leverages the intrinsic splitting effect of optical vortices for a simple and direct analysis of their phase topology. Our method, supported by both experimental results and computational modeling, enables the unambiguous determination of the magnitude and sign of the topological charge without the need for additional optical elements. This is achieved by using an electrically switchable nematic liquid crystal (NLC) Fresnel lens, which we have developed. This lens's tunability and dynamic reconfigurability offer a compact, low-power, and scalable solution for real-time vortex characterization, with potential applications in optical communication, laser beam shaping and structured light applications, quantum photonic technologies, cryptography, and quantum computing.

Results

The Electrically Tunable NLC Fresnel Lens

A design of the proposed nematic liquid crystal Fresnel lens (Figure 1) is based on the domain orientation of the liquid crystal director. To set the initial orientation topology of the LC director (refractive index modulation), a photosensitive film *3* of AtA-2 azo dye (20-30 nm thick) with an absorption band of 450-520 nm was deposited to both glass substrates *1*, pre-coated with a layer of conductive indium tin oxide (ITO) *2* for electrical control of the optical properties of the element [46, 47]. Further, the orienting films on both substrates were exposed to linearly polarized radiation with a wavelength of 450 nm to set boundary conditions for a uniform planar orientation of the NLC director. Due to the reversibility of the orienting properties of AtA-2 azo dye, it is possible to re-irradiate the substrate with radiation with the direction of polarization rotated 90 degrees relative to the initial direction to form a domain structure. To create a structured element, re-exposure was carried out through an amplitude photomask, which is a Fresnel zone plate (15 pairs of concentric rings) with transparent even zones (the radius of the first transparent ring is 473 μm) and opaque odd zones (the radius of the first opaque ring is 333 μm). As a result, boundary

conditions were set on the surfaces of the azo dye films (Figure 1b) for the formation of domains with a twist (the director rotates 90 degrees in the NLC layer) and planar (the director orientation is parallel and coincides on both substrates) director orientations in the nematic liquid crystal layer. The element was filled with a nematic liquid crystal in an isotropic phase after gluing the prepared substrates using fiber spacers with a diameter of 20 μm along the element's edges. Using the technology described above and in Supplementary Note 1, a diffraction grating with planar and twisted director orientation topologies was produced, which is an electrically switchable Fresnel NLC lens.

Previously, the twist-planar topology of the orientation of the NLC director was set using films of polymers (with absorption bands in ultraviolet) or azo dyes (sensitive in the blue region of the spectrum) [48–50]. As practice shows, using photoorientants with an absorption band in the blue region of the spectrum significantly simplifies the process of manufacturing NLC elements. In the current work, the activating dose of AtA-2 azo dye was 0.3 J cm^{-2}, which is an order of magnitude less than the activation dose (5 J cm^{-2}) of polyimide dye PI-3744 in the work [50].

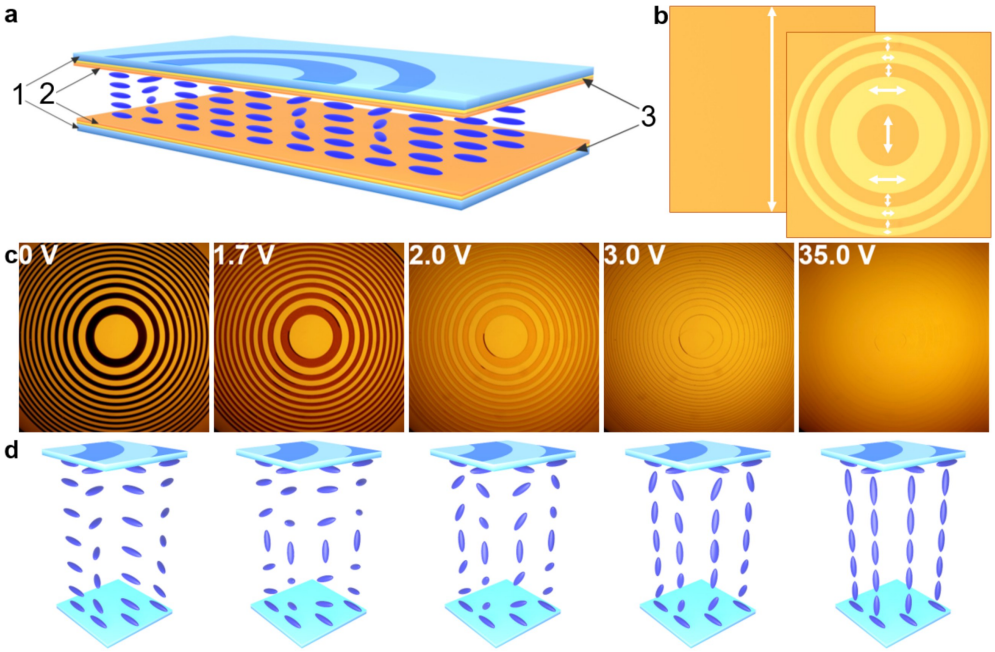

Fig. 1 | Scheme of the NLC Fresnel lens. a, Schematic diagram of the element with the orientation distribution of the liquid crystal director in the twist-planar oriented domains. **b**, Design of boundary conditions for the director of an NLC layer. The arrows schematically indicate the liquid crystal director's directions. **c**, Experimental micrographs of the electrically controlled NLC Fresnel lens placed between parallel polarizer and analyzer at different control voltage values U: from 0 V to 35 V (from left to right) and **d**, the corresponding distribution of NLC molecules.

The pronounced electro-optical response (modulation of the anisotropy of the refractive index $\Delta n(U)$) of a nematic liquid crystal makes it possible to effectively control the properties of the manufactured structure using an external electric voltage applied to the electrodes of the cell (Figure 1c, d). In the voltage range from 0 V to 1.5 V, the twist-planar structure consists of two independent thin amplitude grids of rectangular stroke profile [51, 52]. Twist-oriented LC domains rotate the plane of polarization of transmitted radiation by an angle of 90 degrees. The study of a structured lens by polarizing microscopy in the case when the lens was placed between a parallel polarizer and analyzer showed that areas with a twisted structure correspond to dark areas, and areas with a uniform planar orientation correspond to light areas. The supply of an external control voltage to the electrodes of the NLC element above the threshold value (U_{th} = 1.1 V) causes an electro-optical response, which is expressed in the aspiration of the molecules to reorient along the lines of force of the electric field (Fredericks transition [53, 54]). When the voltage reaches a value corresponding to the optical threshold (U_{op} = 1.5 V), the Mogen condition [55] is disrupted in domains with a twist-oriented director due to the formation of a region with homeotropically arranged molecules and an indefinite azimuthal angle in the center of the LC layer parallel to the glass substrates. The reorientation leads to the transformation of amplitude gratings into a phase sinusoidal diffraction structure with a maximum value of diffraction efficiency (30% [51]) at a control voltage value of the order of 3 V. When the voltage reaches 35 V, the diffraction structure unwinds and the domain structure disappears (all NLC layer molecules are homeotropically oriented) [56].

Determinaton of the Phase Topology of a Singular Beam

To study the phase topology of optical vortices after passing through a twist-planarly oriented NLC Fresnel lens, we constructed an experimental setup shown in Figure 2b and described in detail in Supplementary Note 2. The set-up consists of a radiation source He-Ne laser wavelength of 632.8 nm, collimating system which consist of an objective 20X and lens with focusing distance of 20cm to form a phase singular beam using a phase plate. The formed optical vortex with a topological charge ℓ evolves through the focusing NLC Fresnel lens (the optical axis of the singular beam passes through the center of the Fresnel lens). It is recorded by the charge-coupled device (CCD) behind the NLC element. Patterns of intensity distribution profiles were then imaged with the CCD camera and analysed on the computer.

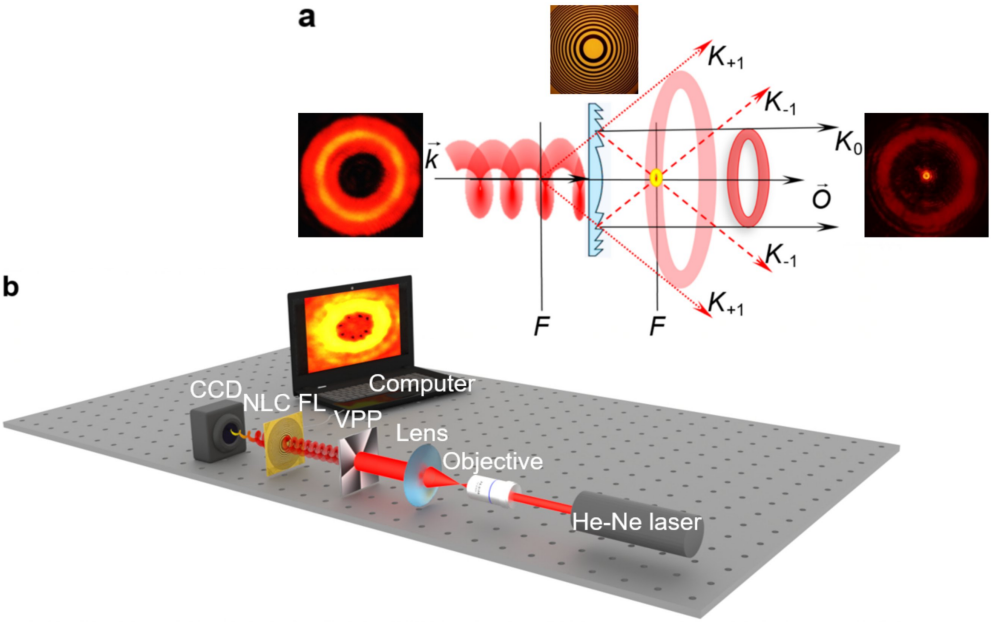

Fig. 2 | Schematics to analyze singular beams. a, Analysis and principle of determination of the phase topology and instability of optical vortices with NLC twist-planar Fresnel lens. **b**, The experimental setup to study the distribution profile of an optical vortex, with a He-Ne laser $\lambda = 632.8$ nm, a 20X objective, a spherical lens, a vortex phase plate (VPP), a NLC Fresnel lens (NLC FL), a CCD camera, a computer.

Figure 3 shows experimental evidence of the normal centrosymmetric passage of an optical vortex with an integer topological charge through a nematic liquid crystal twist-planar oriented Fresnel lens in the focal plane of the element. A ℓ-multiply degenerate intensity zero decays into ℓ isolated first-order intensity zeros located in the central region of the phase singular beam (Figure 3, $\theta = 0$ degrees). When the Fresnel lens is rotated around the vertical axis (changing the angle of incidence of radiation), an astigmatic transformation of the optical vortex occurs and ℓ isolated intensity zeros are observed (Figure 3, $\pm\theta$) lying on a straight line in the transverse plane at an angle of ± 45 degrees to the plane of astigmatism, depending on the sign of the topological charge ℓ of the initial optical vortex. A positive charge ($\ell > 0$) corresponds to an angle of $+45$ degrees, and a negative charge ($\ell < 0$) corresponds to an angle of -45 degrees. Phase singular beams with topological charges ℓ from ± 1 to ± 8 have been experimentally analyzed. Experimental results and numerical simulation when an external control voltage is applied to a Fresnel NLC lens are shown in Supplementary Notes 2 and 4, accordingly.

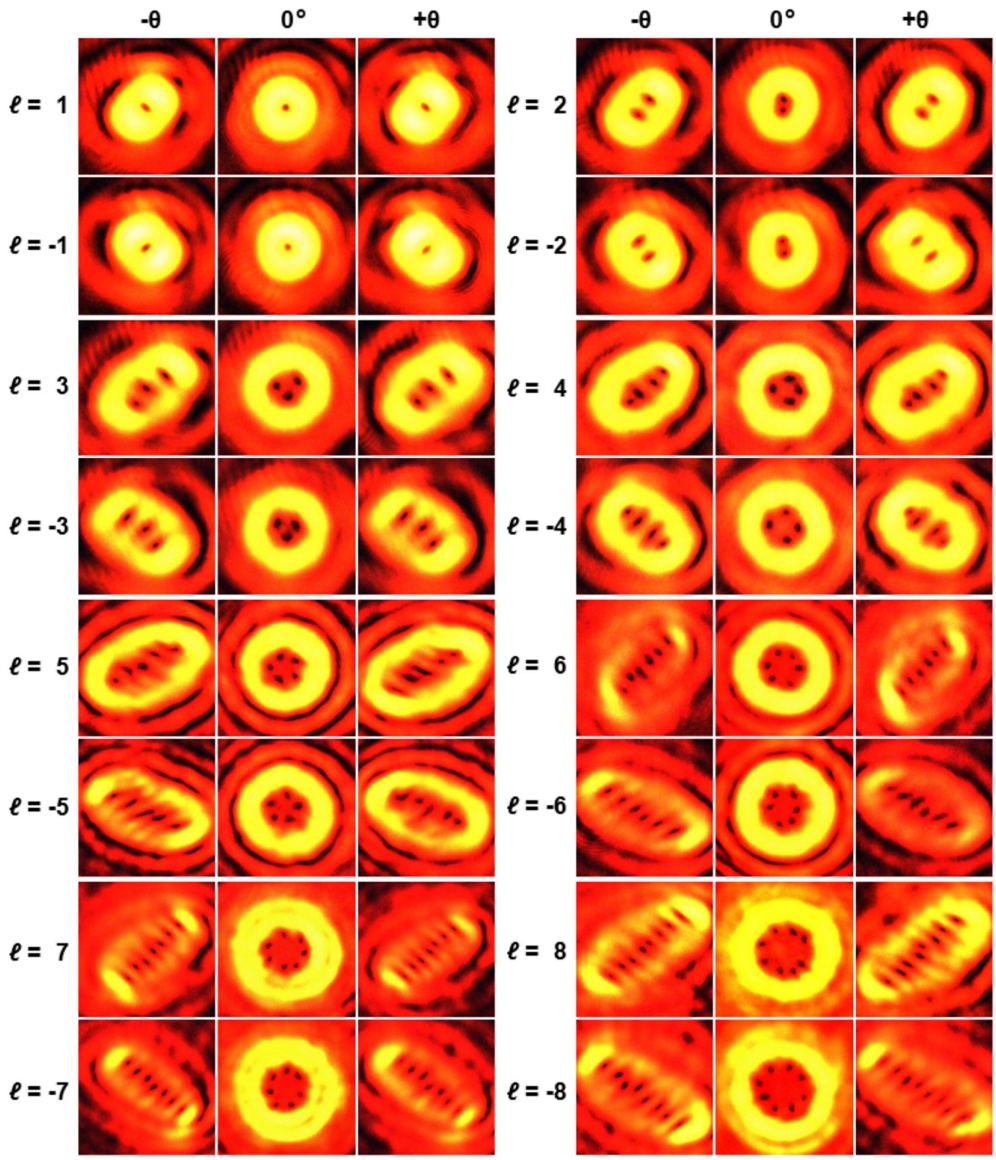

Fig. 3 | Experimental characterization of the phase topology of OVs. The distribution profile of the light field of a phase singular beam with topological charges ℓ from ± 1 to ± 8 in the focal plane of the Fresnel lens: under normal incidence of an optical vortex on the NLC lens ($\theta = 0$ degrees) and when the radiation incidence at angles of $-\theta$ and $+\theta$ (θ increased from 9 to 18 degrees with increasing topological charge) to the normal of the lens.

For a beam with a topological charge of ℓ = -2, the intensity distributions in the focal plane when slightly changing the angle of incidence of radiation on the NLC lens from 0 (normal incidence) to 10 degrees in 2 degree increments (Figure 4) are analyzed. The obtained experimental results (Figure 4a) agree well with theoretical

analyses (Figure 4b). The number of intensity dips is equal to the order (magnitude of the topological charge) of phase singular beam. Moreover, the sign of the charge is easily distinguished. As the angle of incidence of the studied radiation on the lens changes, the orientation of the light field distribution profile changes accordingly: modulated into elliptical and tilted distribution.

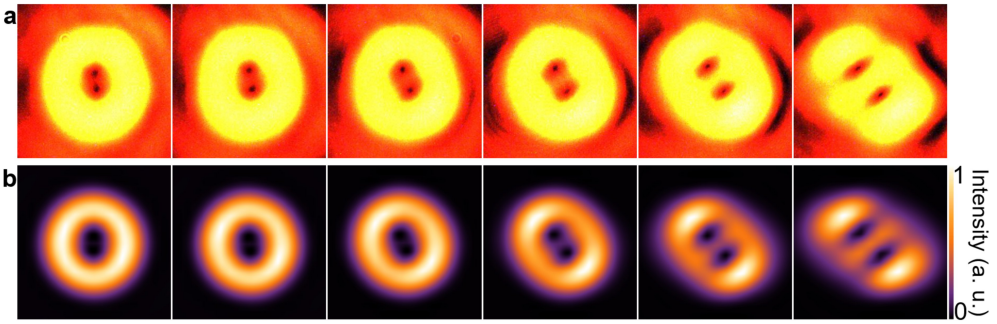

Fig. 4 | Experimental and numerical research of the Phase Topology of OVs. Experimental (**a**) and theoretical (**b**) results of the light field distribution profile of a phase singular beam with a topological charge ℓ = -2 in the focal plane of the Fresnel lens when the angle of incidence θ of radiation on the lens changes: from 0 to +10 degrees in increments of 2 degrees.

Figure 5 shows the experimental results of a study of focusing a phase singular beam with a topological charge of $|\ \ell\ | = 3$ by the NLC Fresnel lens at different values of the external control voltage applied to the lens. An analysis of the distribution profile of the optical vortex light field in the focal plane of the NLC lens showed that when a phase singular beam is diffracted on the NLC Fresnel lens, an optical vortex is observed in the direction of 0 diffraction order (direct radiation – Figure 2a, K_0) and radiation in the direction of -1 diffraction order (converging wave – Figure 2a, K_{-1}). The nonmonotonic dependence of the focusing properties of the manufactured element is shown. The diffraction efficiency is maximal at a voltage of about 3 V (the optimal voltage value [56]) and we observe the absence of radiation in the direction of the diffraction order 0 (K_0). With a further increase of the value of the external voltage on the element, a monotonous decrease in diffraction efficiency is observed, due to the reorientation of liquid crystal molecules along the lines of electric field strength. Thus, the supply of the external control voltage of the order of 35 V (turning off the diffraction mode of operation of the NLC lens) makes it possible to realize the transmission mode of the incoming optical signal without removing the NLC Fresnel lens from the circuit.

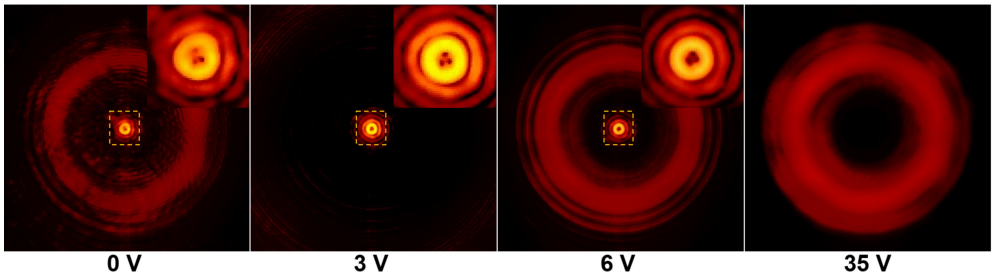

Fig. 5 | Electrical switching of the NLC lens operation modes. The distribution profile of the light field of the phase singular beam with a topological charge of $|\ell| = 3$ in the focal plane of the Fresnel lens under normal incidence of the optical vortex on the NLC lens at different values of the control voltage (U): from 0 V to 35 V (from left to right). The inserts show enlarged images of the selected areas of the photos.

Figure 6 illustrates the theoretical (Figure 6a-c) and experimental (Figure 6a′-a‴, b′-b‴, c′-c‴) results of analyzing the distribution profile of the converging wave in the -1 diffraction order direction as radiation propagates: before focus (Figure 6a-a‴), in focus (Figure 6b-b‴) and after focus (Figure 6c-c‴). It is shown that an optical vortex with a charge of $\ell = +3$ is unstable in real conditions, as a result of which it splits into 3 separate vortices in the focal plane of the lens (Figure 6b′-b‴). The experiment was also performed with a spherical lens with the same focal length. The results obtained with its help (Figure 6a‴-c‴) are qualitatively identical to the results obtained using the Fresnel lens (Figure 6a′-c′, a″-c″). The study of the phase topology of optical vortices by coherent addition with spherical and plane waves is presented as Supplementary Note 3.

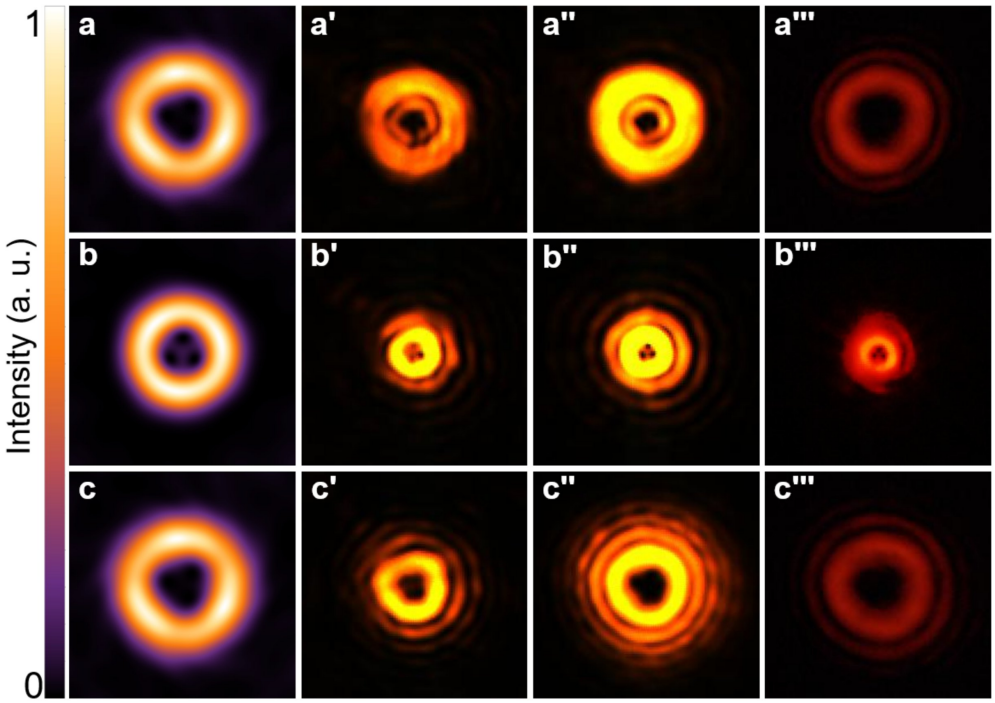

Fig. 6 | Experimental and numerical investigation of the phase topology of OVs near the Fourier plane. Light field distribution profile of a phase singular beam with a topological charge ℓ=+3: 2 cm before (**a-a**$'''$), in (**b-b**$'''$) and 2 cm after (**c-c**$'''$) the focal plane of the lens. **a-c, a**$'$**-c**$'$, corresponds to use of Fresnel lens with control voltage $U = 0$ V and **a**$''$**-c**$''$, with $U = 3$ V. **a**$'''$**-c**$'''$, corresponds to use spherical lens.

Discussion

Optical vortices hold immense promise for next-generation photonic technologies, offering new avenues for communication, computation, and material processing [1, 2]. However, their full potential remains untapped due to persistent technical challenges. As is known, the presence of noise in a singular light field leads to the decay of high-order optical vortices into several vortices with a charge $\mid \ell \mid = 1$, for example, in the presence of a coherent background [57]. Thus, under real conditions, Laguerre-Gaussian beams with a topological charge $\mid \ell \mid > 1$ persist over limited distances and disintegrate in the presence of noise. The decay of a high-order singular phase beam into optical vortices with single charges $\mid \ell \mid = 1$ [33, 35] with the preservation of the total topological charge is due to the presence of noise caused by the imperfection of optical elements with which the corresponding phase transformation is carried out (optical phase plates with smoothly variable thickness, spatial LC light modulators, holographic elements, q-plates, etc.).

The main non-resonator elements for vortex formation are phase isotropic elements with spirally varying material thickness [39, 58, 59] and q-plates - anisotropic centrally symmetric azimuthally structured optical elements [26, 60, 61]. The fabrication of

such elements requires overcoming the problems of design accuracy and technological limitations associated with the high precision of positioning the center of the element (with an accuracy of less than 1 μm) around which the optical properties change.

Another technology for creating phase singular beams is the use of spatial liquid crystal light modulators [39, 58, 59]. However, the limitation of spatial resolution (for example, the pixel size of 3.74 μm (EXULUS-4K1, Thorlabs)), phase shift discretization, and the presence of pixel spacing lead to a deterioration in the quality of the generated beam.

The technological and constructive disadvantages of the described methods of forming singular phase fields lead to the fact that in realistic scenarios, vortexes are unstable and disintegrate when propagating in free space. A CCD camera is usually used to analyze the evolution of vortices in an experiment, moving it along the beam propagation axis to control the intensity distribution in its cross section. However, the distance to which the camera can be moved is limited by the possibility of experimental conditions. In this regard, the qualitative analysis of the far zone for assessing the stability of optical vortices becomes a rather serious task that needs to be solved. Addressing the unmet needs of phase topology stability is critical for realizing the transformative impact of optical vortices in both fundamental research and real-world applications. As a solution, we propose using a focusing lens to transfer the intensity distribution of the light field from the Fraunhofer zone to the Fourier zone. The Fourier transform using a lens allows for an effective analysis of the stability of phase singular beams (Figures 3, 6, Supplementary Note 4).

Interference methods [38, 62–64] are traditionally used to determine the topological charge of optical vortices, requiring complex optical circuits with multiple elements to produce a coherent plane or spherical wave. However, the need for a coherent reference wave, the presence of aberrations, defects in optical elements, and alignment errors can significantly distort the interference pattern, make it difficult to determine the topological charge, and limit practical applications. This stimulated the development of alternative approaches to the characterization of optical vortices. In recent years, diffraction methods [65–68] for determining topological charge have been actively developing, which have a number of advantages over interference methods. They require fewer optical elements and are more resistant to external influences. At the same time, diffraction methods make it possible to carry out measurements in real time without the need for complex adjustment of the optical circuit and without using a coherent reference wave. However, despite the large number of methods already developed, they all have some limitations and difficulties in implementation. Therefore, at present, determining the phase topology of optical vortices is one of the key tasks of modern photonics to expand the field of application of phase singular beams.

We propose using the effect of "splitting" an optical vortex with a charge ℓ in the far zone into $\mid \ell \mid$ separate regions of zero intensity as a new effective and simple method for determining the topological charge of a phase singular beam (Figure 3). Hence, the generation of $\mid \ell \mid$ isolated intensity zeros in the focal plane of a spherical and the NLC Fresnel lenses when a phase singular beam with topological charge ℓ passes through it has been numerically and experimentally demonstrated (Figures

3, 6, Supplementary Notes 2, 3, 4). The addition of astigmatism to the beam by rotating the lens leads to alignment of the formed intensity zeros along a straight line at an angle of ±45 degrees to the plane of the introduced astigmatism (Figures 3, 4, Supplementary Notes 2, 4). When the topological charge is positive, the angle will be +45 degrees and when the charge is negative, it will be −45 degrees. We also suggest using the NLC Fresnel lens as a focusing element (Figure 1, Supplementary Note 1). The use of the LC lens allows for electrical switching of the "optical singular beam propagation" and "topological charge detection" modes in real time without changing the optical circuit (Figure 5).

Acknowledgements. The research was supported by the Israel Science Foundation (ISF) - no. 1023/24 and the state program of scientific research of Belarus "Convergence-2025".

References

[1] Padgett, M.J.: Orbital angular momentum 25 years on. Optics express **25**(10), 11265–11274 (2017)

[2] Shen, Y., Wang, X., Xie, Z., Min, C., Fu, X., Liu, Q., Gong, M., Yuan, X.: Optical vortices 30 years on: Oam manipulation from topological charge to multiple singularities. Light: Science & Applications **8**(1), 90 (2019)

[3] Huang, J., Mao, J., Li, X., Yuan, J., Zheng, Y., Zhai, C., Dai, T., Fu, Z., Bao, J., Yang, Y., et al.: Integrated optical entangled quantum vortex emitters. Nature Photonics, 1–8 (2025)

[4] Session, D., Jalali Mehrabad, M., Paithankar, N., Grass, T., Eckhardt, C.J., Cao, B., Gustavo Suárez Forero, D., Li, K., Alam, M.S., Watanabe, K., et al.: Optical pumping of electronic quantum hall states with vortex light. Nature Photonics, 1–6 (2025)

[5] Hu, Z., Bongiovanni, D., Wang, Z., Wang, X., Song, D., Xu, J., Morandotti, R., Buljan, H., Chen, Z.: Topological orbital angular momentum extraction and twofold protection of vortex transport. Nature Photonics, 1–8 (2025)

[6] Hu, J., Eriksson, M., Gigan, S., Fickler, R.: Generalized angle–orbital angular momentum talbot effect and modulo mode sorting. Nature Photonics, 1–8 (2025)

[7] Chen, B., Zhou, Y., Liu, Y., Ye, C., Cao, Q., Huang, P., Kim, C., Zheng, Y., Oxenløwe, L.K., Yvind, K., *et al.*: Integrated optical vortex microcomb. Nature Photonics **18**(6), 625–631 (2024)

[8] Krenn, M., Fickler, R., Fink, M., Handsteiner, J., Malik, M., Scheidl, T., Ursin, R., Zeilinger, A.: Communication with spatially modulated light through turbulent air across vienna. New Journal of Physics **16**(11), 113028 (2014)

[9] Richardson, D.J., Fini, J.M., Nelson, L.E.: Space-division multiplexing in optical fibres. Nature photonics **7**(5), 354–362 (2013)

[10] Willner, A.E., Huang, H., Yan, Y., Ren, Y., Ahmed, N., Xie, G., Bao, C., Li, L., Cao, Y., Zhao, Z., *et al.*: Optical communications using orbital angular momentum beams. Advances in optics and photonics **7**(1), 66–106 (2015)

[11] Bruce, G.D., Rodríguez-Sevilla, P., Dholakia, K.: Initiating revolutions for optical manipulation: the origins and applications of rotational dynamics of trapped particles. Advances in Physics: X **6**(1), 1838322 (2021)

[12] Aleksanyan, A., Kravets, N., Brasselet, E.: Multiple-star system adaptive vortex coronagraphy using a liquid crystal light valve. Physical review letters **118**(20), 203902 (2017)

[13] Aleksanyan, A., Brasselet, E.: High-charge and multiple-star vortex coronagraphy from stacked vector vortex phase masks. Optics Letters **43**(3), 383–386 (2018)

[14] Foo, G., Palacios, D.M., Swartzlander Jr, G.A.: Optical vortex coronagraph. Optics letters **30**(24), 3308–3310 (2005)

[15] Serabyn, E., Mawet, D., Burruss, R.: An image of an exoplanet separated by two diffraction beamwidths from a star. Nature **464**(7291), 1018–1020 (2010)

[16] Masuda, K., Nakano, S., Barada, D., Kumakura, M., Miyamoto, K., Omatsu, T.: Azo-polymer film twisted to form a helical surface relief by illumination with a circularly polarized gaussian beam. Optics Express **25**(11), 12499–12507 (2017)

[17] Takahashi, F., Miyamoto, K., Hidai, H., Yamane, K., Morita, R., Omatsu, T.: Picosecond optical vortex pulse illumination forms a monocrystalline silicon needle. Scientific reports **6**(1), 21738 (2016)

[18] Otsu, T., Ando, T., Takiguchi, Y., Ohtake, Y., Toyoda, H., Itoh, H.: Direct evidence for three-dimensional off-axis trapping with single laguerre-gaussian beam. Scientific reports **4**(1), 4579 (2014)

[19] Tan, P., Yuan, X.-C., Yuan, G., Wang, Q.: High-resolution wide-field standing-wave surface plasmon resonance fluorescence microscopy with optical vortices. Applied Physics Letters **97**(24) (2010)

[20] Zhang, C., Min, C., Du, L., Yuan, X.-C.: Perfect optical vortex enhanced surface plasmon excitation for plasmonic structured illumination microscopy imaging. Applied Physics Letters **108**(20) (2016)

[21] Nye, J.F., Berry, M.V.: Dislocations in wave trains. Proceedings of the Royal Society of London. A. Mathematical and Physical Sciences **336**(1605), 165–190 (1974)

[22] Beijersbergen, M., Coerwinkel, R., Kristensen, M., Woerdman, J.: Helical-wavefront laser beams produced with a spiral phaseplate. Optics communications **112**(5-6), 321–327 (1994)

[23] Sueda, K., Miyaji, G., Miyanaga, N., Nakatsuka, M.: Laguerre-gaussian beam generated with a multilevel spiral phase plate for high intensity laser pulses. Optics express **12**(15), 3548–3553 (2004)

[24] Marrucci, L.: The q-plate and its future. Journal of Nanophotonics **7**(1), 078598–078598 (2013)

[25] Melnikova, E., Tolstik, A., Gorbach, D., Stanevich, V.Y., Kukhta, I., Chepeleva, D., Murauski, A.A., Muravsky, A.A.: Achromatic switchable liquid-crystal twist-q-plate. Journal of Applied Spectroscopy **90**(2), 427–435 (2023)

[26] Marrucci, L., Karimi, E., Slussarenko, S., Piccirillo, B., Santamato, E., Nagali, E., Sciarrino, F.: Spin-to-orbital optical angular momentum conversion in liquid crystal "q-plates": Classical and quantum applications. Molecular Crystals and Liquid Crystals **561**(1), 48–56 (2012)

[27] Kobashi, J., Yoshida, H., Ozaki, M.: Broadband optical vortex generation from patterned cholesteric liquid crystals. Molecular Crystals and Liquid Crystals **646**(1), 116–124 (2017)

[28] Ostrovsky, A.S., Rickenstorff-Parrao, C., Arrizón, V.: Generation of the "perfect" optical vortex using a liquid-crystal spatial light modulator. Optics letters **38**(4), 534–536 (2013)

[29] Mirhosseini, M., Magana-Loaiza, O.S., Chen, C., Rodenburg, B., Malik, M., Boyd, R.W.: Rapid generation of light beams carrying orbital angular momentum. Optics express **21**(25), 30196–30203 (2013)

[30] Hwang, M.-S., Kim, H.-R., Kim, J., Yang, B.-J., Kivshar, Y., Park, H.-G.: Vortex nanolaser based on a photonic disclination cavity. Nature Photonics **18**(3), 286–293 (2024)

[31] Bazhenov, V.Y., Vasnetsov, M., Soskin, M.: Laser beams with screw dislocations in their wavefronts. Jetp Lett **52**(8), 429–431 (1990)

[32] Heckenberg, N., McDuff, R., Smith, C., White, A.: Generation of optical phase singularities by computer-generated holograms. Optics letters **17**(3), 221–223 (1992)

[33] Basistiy, I., Bazhenov, V.Y., Soskin, M., Vasnetsov, M.V.: Optics of light beams with screw dislocations. Optics communications **103**(5-6), 422–428 (1993)

[34] Berry, M.V., Dennis, M.R.: Knotted and linked phase singularities in monochromatic waves. Proceedings of the Royal Society of London. Series A: Mathematical, Physical and Engineering Sciences **457**(2013), 2251–2263 (2001)

[35] Ricci, F., Löffler, W., Van Exter, M.: Instability of higher-order optical vortices analyzed with a multi-pinhole interferometer. Optics express **20**(20), 22961–22975 (2012)

[36] Abramochkin, E., Volostnikov, V.: Beam transformations and nontransformed beams. Optics Communications **83**(1-2), 123–135 (1991)

[37] Vaity, P., Banerji, J., Singh, R.: Measuring the topological charge of an optical vortex by using a tilted convex lens. Physics letters a **377**(15), 1154–1156 (2013)

[38] Denisenko, V., Shvedov, V., Desyatnikov, A.S., Neshev, D.N., Krolikowski, W., Volyar, A., Soskin, M., Kivshar, Y.S.: Determination of topological charges of polychromatic optical vortices. Optics express **17**(26), 23374–23379 (2009)

[39] Forbes, A., Dudley, A., McLaren, M.: Creation and detection of optical modes with spatial light modulators. Advances in optics and photonics **8**(2), 200–227 (2016)

[40] Kotlyar, V., Khonina, S., Soifer, V.: Light field decomposition in angular harmonics by means of diffractive optics. Journal of modern optics **45**(7), 1495–1506 (1998)

[41] Dai, K., Gao, C., Zhong, L., Na, Q., Wang, Q.: Measuring oam states of light beams with gradually-changing-period gratings. Optics letters **40**(4), 562–565 (2015)

[42] Guo, C.-S., Yue, S.-J., Wei, G.-X.: Measuring the orbital angular momentum of optical vortices using a multipinhole plate. Applied Physics Letters **94**(23) (2009)

[43] Anderson, M.E., Bigman, H., Araujo, L.E., Chaloupka, J.L.: Measuring the topological charge of ultrabroadband, optical-vortex beams with a triangular aperture. Journal of the Optical Society of America B **29**(8), 1968–1976 (2012)

[44] Leach, J., Padgett, M.J., Barnett, S.M., Franke-Arnold, S., Courtial, J.: Measuring the orbital angular momentum of a single photon. Physical review letters **88**(25), 257901 (2002)

[45] Frączek, E., Frączek, W., Masajada, J.: The new method of topological charge determination of optical vortices in the interference field of the optical vortex interferometer. Optik **117**(9), 423–425 (2006)

[46] Mikulich, V., Murawski, A.A., Muravsky, A.A., Agabekov, V.: Influence of methyl substituents on azo-dye photoalignment in thin films. Journal of Applied

Spectroscopy **83**, 115–120 (2016)

[47] Muravsky, A., Murauski, A., Kukhta, I.: Photoinduced hole dipoles' mechanism of liquid crystal photoalignment. Applied Optics **59**(17), 5102–5107 (2020)

[48] Kazak, A., Tolstik, A., Mel'nikova, E.: Controlling light fields by means of liquid-crystal diffraction elements. Journal of Optical Technology **77**(7), 461–462 (2010)

[49] Chigrinov, V., Sun, J., Wang, X.: Photoaligning and photopatterning: New lc technology. Crystals **10**(4), 323 (2020)

[50] Wang, X.-Q., Srivastava, A.K., Chigrinov, V.G., Kwok, H.-S.: Switchable fresnel lens based on micropatterned alignment. Optics Letters **38**(11), 1775–1777 (2013)

[51] Melnikova, E., Stashkevich, I., Rushnova, I., Tolstik, A., Timofeev, S.: Polarization properties of the electrically controlled twist-planar liquid crystal di. raction structure. Nonlinear Phenomena in Complex Systems **25**(3), 229–244 (2022)

[52] Węgłowski, R., Kozanecka-Szmigiel, A., Piecek, W., Konieczkowska, J., Schab-Balcerzak, E.: Electro-optically tunable diffraction grating with photoaligned liquid crystals. Optics Communications **400**, 144–149 (2017)

[53] Zhou, H., Choate, E.P., Wang, H.: Optical fredericks transition in a nematic liquid crystal layer. Liquid Crystalline Polymers: Volume 2–Processing and Applications, 265–295 (2015)

[54] Lucchetti, L., Catani, L., Simoni, F.: Light-controlled electric freedericksz threshold in dye doped liquid crystals. Journal of Applied Physics **115**(20) (2014)

[55] Mauguin, C.: Sur les cristaux liquides de m. lehmann. Bulletin de Minéralogie **34**(3), 71–117 (1911)

[56] Mel'nikova, E., Panteleeva, E., Gorbach, D., Tolstik, A., Rushnova, I., Kabanova, O.: Electrically controlled liquid crystal twist-planar fresnel lens. Journal of Applied Spectroscopy, 1–6 (2024)

[57] Soskin, M., Gorshkov, V., Vasnetsov, M., Malos, J., Heckenberg, N.: Topological charge and angular momentum of light beams carrying optical vortices. Physical Review A **56**(5), 4064 (1997)

[58] Ma, H., Hu, H., Xie, W., Xu, X.: Study on the generation of a vortex laser beam by using phase-only liquid crystal spatial light modulator. Optical Engineering **52**(9), 091721–091721 (2013)

[59] Szatkowski, M., Masajada, J., Augustyniak, I., Nowacka, K.: Generation of composite vortex beams by independent spatial light modulator pixel addressing. Optics Communications **463**, 125341 (2020)

[60] Nersisyan, S., Tabiryan, N., Steeves, D.M., Kimball, B.R.: Fabrication of liquid crystal polymer axial waveplates for uv-ir wavelengths. Optics express **17**(14), 11926–11934 (2009)

[61] Slussarenko, S., Murauski, A., Du, T., Chigrinov, V., Marrucci, L., Santamato, E.: Tunable liquid crystal q-plates with arbitrary topological charge. Optics express **19**(5), 4085–4090 (2011)

[62] Courtial, J., Dholakia, K., Robertson, D., Allen, L., Padgett, M.: Measurement of the rotational frequency shift imparted to a rotating light beam possessing orbital angular momentum. Physical review letters **80**(15), 3217 (1998)

[63] Harris, M., Hill, C., Tapster, P., Vaughan, J.: Laser modes with helical wave fronts. Physical Review A **49**(4), 3119 (1994)

[64] Cui, S., Xu, B., Luo, S., Xu, H., Cai, Z., Luo, Z., Pu, J., Chávez-Cerda, S.: Determining topological charge based on an improved fizeau interferometer. Optics express **27**(9), 12774–12779 (2019)

[65] Melo, L.A., Jesus-Silva, A.J., Chávez-Cerda, S., Ribeiro, P.H.S., Soares, W.C.: Direct measurement of the topological charge in elliptical beams using diffraction by a triangular aperture. Scientific Reports **8**(1), 6370 (2018)

[66] Han, Y., Zhao, G.: Measuring the topological charge of optical vortices with an axicon. Optics letters **36**(11), 2017–2019 (2011)

[67] Izdebskaya, Y.V., Rebling, J., Desyatnikov, A.S., Kivshar, Y.S.: Observation of vector solitons with hidden vorticity. Optics Letters **37**(5), 767–769 (2012)

[68] Mesquita, P.H., Jesus-Silva, A.J., Fonseca, E.J., Hickmann, J.M.: Engineering a square truncated lattice with light's orbital angular momentum. Optics express **19**(21), 20616–20621 (2011)

[69] Muravsky, A.A., Murauski, A.A., Kukhta, I.N., Yakovleva, A.S.: High anchoring photoalignment material based on new photo-induced hole dipoles' mechanism. Journal of the Society for Information Display **29**(11), 833–839 (2021)

[70] Melnikova, E., Gorbach, D., Slussarenko Sr, S., Muravsky, A., Tolstik, A., Slussarenko Jr, S.: Liquid-crystal q-plates with a phase core to generation vortex beams with controllable number of singularities. Optics Communications **522**, 128661 (2022)

[71] Melnikova, E.A.: Electrically controlled microstructured liquid-crystal twist elements for phase conversion of light fields. Journal of Optical Technology **89**(3), 169–175 (2022)

[72] Melnikova, E., Pantsialeyeva, Y., Gorbach, D., Tolstik, A., Karabchevsky, A.:

Tunable liquid crystal twisted-planar fresnel lens for vortex topology determination. Laser & Photonics Reviews, 2401006 (2024)

[73] Plick, W.N., Krenn, M.: Physical meaning of the radial index of laguerre-gauss beams. Physical Review A **92**(6), 063841 (2015)

Supplementary Information

1 Fabrication of the Electrically Controlled Twist-Planar Oriented Liquid Crystal Fresnel Lens

The method of manufacturing the NLC Fresnel lens, the structural scheme of which is shown in Figure 1a, b, consists of several successive stages: preparation of glass substrates, deposition of thin films of AtA-2 azo dye on the substrates, photoorientation of AtA-2 azo dye, cell assembly, filling of the cell with nematic liquid crystal.

Substrates Preparation: the corpus of the controlled NLC Fresnel lens was manufactured using 1.1 mm thick glass substrates with a continuous transparent electrically conductive indium tin oxide (ITO) coating with a resistance of 100 Ohm square^{-1} on the inner surface (INTEGRAL OJSC, Minsk, Belarus). A diamond roller glass cutter (Bohle AG) was used to prepare the substrates of the required size (20x30 mm) and shape.

The pre-cleaning of the substrate surfaces took place in an ultrasonic bath: once in a solution of a surfactant with distilled water at a temperature of T = 45°C for 15 minutes; then two times in distilled water at a temperature of T = 45°C for 15 minutes. The next step was to clean the glass substrates with a cotton textile soaked in isopropyl alcohol. The substrates are then dried with a second clean, dry cotton textile. At this stage of cleaning, dust particles and lint from the cleaning cloth are allowed on the glass (dirt and stains should not be present). To remove foreign particles from the substrate surface, they are blown with a jet of compressed air using a compressor (Remeza CJSC, Minsk, Belarus).

To check the degree of purification, two substrates are pressed tightly against each other with their work surfaces inside, and interference fringes are observed in the light of a table lamp. If there are few of them (2-4), then it is assumed that there are no foreign particles and dirt on the work surfaces. Otherwise, it is necessary to repeat the process of cleaning the working surfaces of glass substrates.

Organic pollutants were removed using a UV cleaning system (Photo Surface Processor PL16-110D, SEN LIGHTS Corp., JP). After application of the system, it is necessary to blow the substrates again with compressed air to remove traces of organic pollutants.

Deposition of AtA-2 Azo Dye Thin Films to Substrates: to deposite thin (about 30 nm) films of photoorienting material (AtA-2 azo dye synthesized in the Laboratory of Materials and Technologies of LC Devices of the Institute of Chemistry of New Materials of the National Academy of Sciences of Belarus) from liquid solutions to the inner surfaces of purified glass substrates, the method of creating a meniscus with a rod (Mayer-Rod Coating) was used. AtA-2 azo dye has high sensitivity in

the blue region of the spectrum and is characterized by high adhesion energy to LC molecules [46, 69], implements a new mechanism for the orientation of a liquid crystal of "photoinduced hole dipoles" [47]. After deposition, the azo dye must be dried on a hot plate at 140°C for 5 minutes to evaporate the solvent.

Photoorientation of the AtA-2 Azo Dye: azo dye films acquire orienting properties when exposed to linearly polarized light. It is important to note that the direction of the induced orientation of the azo dye molecules is perpendicular to the direction of polarization of the activating radiation. The orientation direction in the AtA-2 azo dye thin film can be easily changed further by additional irradiation with activating radiation with an alternate polarization direction.

The activation of ATA-2 azo dye on the inner surfaces of glass substrates was carried out in two stages [70, 71]. At the first stage, both substrates were uniformly exposed with LED radiation with a wavelength $\lambda = 450$ nm and linear polarization (the power density was I = 15 mW cm^{-2}). At the second stage, a thin film of the photoorientant was re-exposed on only one substrate using an amplitude glass mask and linearly polarized radiation with an orthogonal direction of the radiation polarization vector relative to its direction at the first stage and a power density of I = 45 mW cm^{-2}. The transmission profile of the amplitude glass mask for photoorientation of AtA-2 azo dye corresponded to a Fresnel lens with a radius of the first zone $r_1 = 333$ μm. The mask was made by lithographic technology on OJSC Integral (Minsk, Belarus).

Assembling the Lens Cell: the body of the NLC Fresnel lens was assembled in a laminar flow cabinet equipped with an air flow circulation and purification system in order to avoid repeated contamination of the working surfaces of the glass substrates. The thickness of the homogeneous air gap in the experimental sample was determined by fiber polymer spacers with a diameter of 20 μm located along two opposite edges of the substrates. The glass substrates were glued along the perimeter with UV glue (Norland NOA81, Edmund Optics) from two opposite sides, leaving space on the substrates for voltage supply and cell control.

The formed air gap between the glued substrates makes it possible to fill the element with a nematic liquid crystal by the capillary method under the condition of its isotropic phase at a temperature of 65°C in the drying cabinet (laboratory furnaces SNOL 58/350, AB UMEGA-GROUP Lithuania).

2 Experimental Section

Electrical Control of the Properties of the NLC Fresnel Lens: to obtain the electro-optical response of the NLC layer, which provides effective electrical control of diffraction properties, an alternating voltage of rectangular pulse shape (meander) with a frequency of 1 kHz was applied to the electrodes of the NLC lens using an installation Arbitrary Waveform Generator B-332 (LANFOR Company, St. Petersburg, Russia).

Polarization Microscopy (Figure 1c): the study of the formed anisotropic structure in the NLC layer was carried out on video complex based on polarizing microscope (Optoelectronic Systems OJSC, Minsk, Belarus) with digital camera, resolution of 2560x1920 pixels.

Experimental Systems for Phase Topology Measurements (Figure 2b): in the work, radiation with a wavelength of λ=632.8 nm was used, generated by He-Ne laser LGK 7665 P18 (LASOS Lasertechnik GmbH). The size matching of the laser radiation and the Fresnel LC lens (about 4 mm) was implemented using a collimator consisting of a micro lens (20x) and a focusing lens (f=20cm).

The formation of a phase singular beam with a topological charge ℓ from ± 1 to ± 8 was realized using a Spiral Plate (SP) VPP-m633 (RPC Photonics, Inc.).

Intensity distribution profiles (Figures 2, 3, 4a, 5, 6a′-a‴, b′-b‴, c′-c‴, S1, S2) were recorded using a CCD camera FLIRCHAMELEON CMLN-13S2M-CS (FLIR Integrated Imaging Solutions, Canada).

The experimental results were confirmed using a focusing spherical lens with a focal length of f=17cm (Figure 6a‴- c‴, S2).

Figure S1 shows the experimental results of the astigmatic transformation of an optical vortex with a topological charge $\ell = +3$ at the external control voltage (U) of 0 V and 3 V ("topological charge detection" mode) to the NLC Fresnel lens. It can be seen from the figure that in the absence of rotation of the lens in the Fourier plane, the optical vortex splits into three phase singular beams with topological charges $|\ \ell\ | = 1$. The rotation of the NLC Fresnel lens around the Z axis leads to the alignment of intensity zeros on a straight line. Applying the optimal voltage (3 V) to the NLC element results in an increase in intensity.

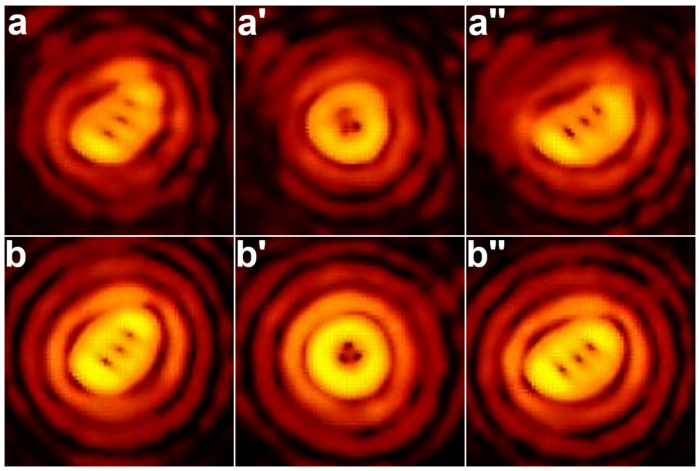

Fig. S1 | Experimental characterization of the phase topology of OVs via NLC Fresnel lens. The distribution profile of the light field of a phase singular beam with topological charge $\ell = +3$ in the focal plane of the Fresnel lens: **a′**, **b′**, under normal incidence of an optical vortex on the NLC lens ($\theta = 0$ degrees) and when the radiation incidence at angles of $\theta = -10$ degrees (**a**, **b**) and $\theta = +10$ degrees (**a″**, **b″**) with control voltage $U = 0$ V (a-a″) and $U = 3$ V (b-b″).

3 Analysis in the Mach-Zehnder Interferometer

A study of the phase topology of the vortex using a Mach-Zehnder interferometer (the method of coherent addition of the studied beam with a spherical (Figure S2b-b′′′′) or plane wave (Figure S2c-c′′′′)) showed a change in the sign of the topological charge of the phase singular beam focused by the lens to the opposite after passing through the focal plane of the lens [72]. The instability of a phase singular beam in the Fourier plane of the spherical lens has also been experimentally shown (Figure S2a′′-c′′).

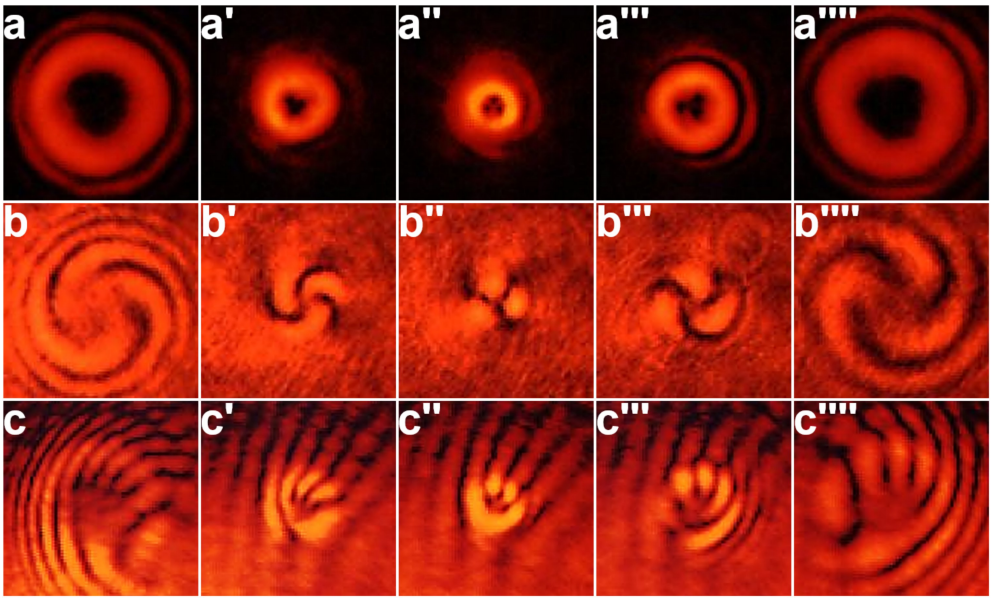

Fig. S2 | Analysis in the Mach-Zehnder interferometer. Light field distribution profile: 2 cm before (**a-c**), 0.6 cm before (**a′-c′**), in (**a′′-c′′**), 0.6 cm after (**a′′′-c′′′**) and 2 cm after (**a′′′′-c′′′′**) the focal plane of the spherical lens. **a-a′′′′**, photographs of optical vortex with a topological charge $\ell = +3$ when passing through a spherical lens. The photographs of the interference pattern of an optical vortex with a spherical wave (b-b′′′′) and a plane wave (c-c′′′′).

4 Numerical Simulations of Vortex Beam Propagation via the NLC Fresnel Lens

The pattern of the distribution profile of the light field of a phase singular beam in the direction of -1 the diffraction order (converging beam, E_{-1}) during the passage of an optical vortex with a topological charge ℓ through a nematic liquid crystal Fresnel lens was analytically calculated using a software system Wolfram Mathematica (Figures 4b, 6a-c, S3).

The amplitude of the electromagnetic field $E_0(\rho, \phi)$ of an optical vortex incident on the NLC Fresnel lens is represented as a superposition of a Laguerre-Gaussian

$E_{LG}(\rho, \phi)$ beam (signal) and Gaussian $E_G(\rho)$ beam (noise) in the following form:

$$E_0(\rho, \phi) = \alpha E_{LG}(\rho, \phi) + \sqrt{1 - \alpha^2} E_G(\rho), \tag{1}$$

where $\rho = \sqrt{x^2 + y^2}$ and $\phi = \arctan(\frac{y}{x})$ are the radial and angular cylindrical coordinates in the transverse plane of the beam, x, y, z – coordinates of the point of the singular beam (the origin of the coordinate system is in the center of the beam), α^2 – signal intensity amplitude (in simulations α is equal to 0.998), $1 - \alpha^2$ – the amplitude of the noise intensity (in simulations equal to 0.4%).

The Laguerre-Gaussian $E_{LG}(\rho, \phi)$ beam at the beam waist position (e.g. $z = 0$) with azimuthal number ℓ, and radial number ρ=0:

$$E_{LG}(\rho, \phi) = C_\ell e^{-\frac{\rho^2}{w_0^2} + i\ell\phi} \frac{1}{w_0} (\frac{\rho}{w_0})^{|\ell|} L_p^{|\ell|} (\frac{2\rho^2}{w_0^2}), \tag{2}$$

where $L_\rho^{|\ell|}$ is the generalized Laguerre polynomial, C_ℓ is the normalization constant, and w_0 is the beam waist [73].

The amplitude of the Gaussian beam $E_G(\rho)$ at $z = 0$ with a beam waist equal to w_G:

$$E_G(\rho) = \frac{e^{-\frac{\rho^2}{w_G^2}} \sqrt{2}}{w_G \sqrt{\pi}}. \tag{3}$$

The beam amplitude at distance z (Figures 6a-c) is simulated by calculating the Fresnel diffraction integral with wavelength λ=632.8 nm:

$$E(x, y, z) = \frac{e^{i2\pi z}}{i\lambda z} e^{i\frac{\pi}{\lambda z}(x^2 + y^2)} \iint_{-\infty}^{+\infty} E_0(x', y') U(x', y') e^{i\frac{\pi}{\lambda z}(x'^2 + y'^2)} e^{-i2\pi(\frac{xx'}{\lambda z} + \frac{yy'}{\lambda z})} dx' dy'. \tag{4}$$

The function $U(x', y')$ is the intensity mask of the Fresnel lens with a focal length f = 17.6 cm:

$$U(x', y') = 1 - \lfloor \frac{x'^2 + y'^2}{\lambda f} mod\ 2 \rfloor. \tag{5}$$

The results of numerical simulation of the distribution profile of an optical vortex diffracted in the -1 direction of the diffraction order (converging beam, E_{-1}) with topological charge ℓ from ± 1 to ± 6 in the focal plane of the Fresnel lens when rotating the NLC element around the vertical axis are shown in the Figure S3. The simulation results are fully consistent with the experimental results (Figure 3).

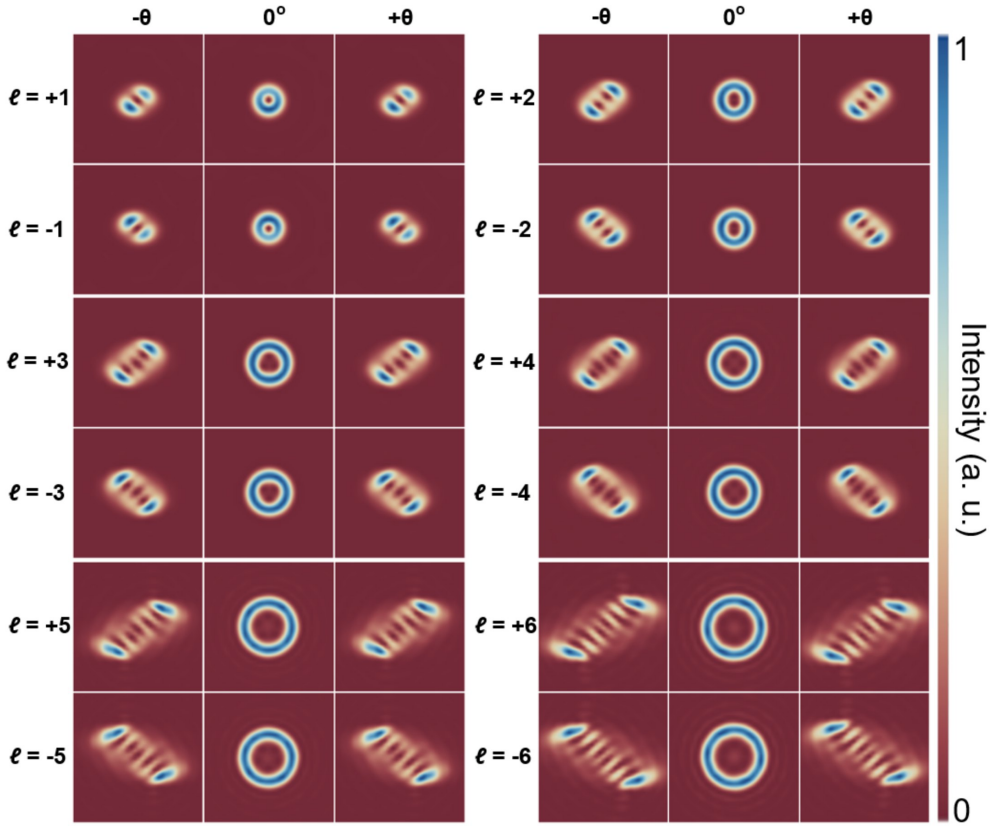

Fig. S3 | Theoretical characterization of the phase topology of OVs. The distribution profile of the light field of a phase singular beam with topological charge ℓ from ± 1 to ± 6 in the focal plane of the Fresnel lens: under normal incidence of an optical vortex on the NLC lens ($\theta = 0$ degrees) and when the radiation incidence at angles of $-\theta$ and $+\theta$ (θ increased from 9 to 18 degrees with increasing topological charge) to the normal of the lens.